

# **BISMUTH OXIDE AND BISMUTH OXIDE DOPED GLASSES FOR OPTICAL AND PHOTONIC APPLICATIONS**

*S. P. Singh and B. Karmakar*

Glass Science and Technology Section, Glass Division, Central Glass and Ceramic Research Institute (CSIR, India), 196, Raja S.C. Mullick Road, Kolkata 700032, India, Tel.: +91- 33 2473 3496: fax: +91- 33 2473 0957., \*E-mail: basudebk@cgcri.res.in.

## **ABSTRACT**

Glasses formed with heavy metal (atomic weight >100) oxides (HMO) have received significant attention because of their interesting physical and optical properties. In this perspective, bismuth (atomic weight = 209) oxide containing glasses is one of the most important members of this family. Bismuth oxide glasses are very useful for exploiting as lead-free, low-softening point, high refractive index, high density and radio shielding glasses. These glasses have long infrared cut-off, which makes them ideal candidates for optical transmission in the infrared to visible region. Thus there has been an increasing interest in the studies of synthesis, microstructure, physical and optical properties of bismuth oxide containing glasses and bismuth oxide doped glasses. Optical absorption studies of bismuth oxide glasses yield important information regarding their electronic states. The synthesis of size-controlled, spherical Bi nanoparticles and strategies for generation of various shaped Bi nanoparticles in glass matrix is again a very attractive area for nanomaterial research. Moreover, the generation of surface plasmon resonance due to various shape and sizes bismuth nanoparticles is yet again open a very fascinating research area for plasmonic, nanophotonic and optoelectronic applications. Recent advances have sparked intense interest in bismuth-doped optical materials. Their broadband photoluminescence near infrared (NIR) has been established in many glasses. The bismuth oxide doped fibre lasers and amplifiers have created up to now to cover the spectral region 1100 to 1550 nm. The current trends show that the bismuth oxide and its doped glasses are very attractive and important optical materials for various scientific as well as technological applications.

## **1. INTRODUCTION**

Recently, glasses containing bismuth oxide have attained great attention, since they are used in the wide area of applications. The obtained glasses are characterized by high density, high refractive index, extended transmission in mid-IR, high dielectric constant, etc. Hence there has been an increasing interest in the synthesis, microstructure and physical properties of heavy metal oxide (HMO) glasses containing bismuth oxide as a major component. Bismuth oxide ( $\text{Bi}_2\text{O}_3$ ) based glasses for their high polarizability has fascinated much attention of glass researchers because of their nonlinear optical properties which have importance for the development of optical information processing technology [1-3]. For this purpose, glasses of higher optical nonlinearity have to be found or designed on the basis of correlation of the optical nonlinearity with some other electronic properties which are easily understandable and accessible. Therefore, many studies on their structure and optical properties have been carried out. Glasses containing heavy metal oxide (HMO) have attracted attention of several researchers for excellent infrared transmission compared with the conventional glasses which make it an ideal candidate for various applications such as infrared transmission components, ultra fast optical switches, and photonic devices. [1-3]. Attempts have been made to explore the mechanical, thermal and optical properties of these glasses. Among the other HMO glasses, bismuth oxide glasses have

wide range of applications in the field of glass ceramics, layers for optical and electronic devices, thermal and mechanical sensors, reflecting windows [4-6]. Lead oxide is widely used as a component in the low melting glasses. But due to its hazardous effect on health and environment, it is being eliminated from various applications [7, 8]. In this context, bismuth oxide is a suitable substitute of lead oxide for its isoelectronic properties. Therefore, bismuth glasses are very useful for exploiting as lead-free low-softening point dielectric glasses for plasma display panel, thick film conductors, sealing glasses for metals, etc. [7,8]. Moreover, lead oxide containing glasses shows extremely high radioactive resistance because of their high density and atomic number. In this context bismuth glasses could also be used as lead-free high density radiation shielding window (RSW) glasses. But the big problem associated with bismuth oxide glasses is its deep brown or black coloring as its concentration and melting temperature increases [9, 10]. Therefore, to obtain very high transmitting bismuth oxide glass is a technological challenge for the glass researchers.

Bismuth oxide cannot be considered as a glass network former due to low field strength (0.53) of  $\text{Bi}^{3+}$  ion. However, in combination with  $\text{B}_2\text{O}_3$  glass former it is possible to obtain glasses in a relatively large compositional ranges. A survey of literature shows that there are many reports available on ternary bismuth borate glasses [11-14]. The properties of the glasses are closely related to inter-atomic forces and potentials in lattice structure. Thus any change in the lattice due to doping can be directly being noticed. The cerium dioxide, copper oxide and iron oxide can be used as a dopant in the bismuth glasses to remove its deep brown coloring as well as to improve its other optical, electrical and magnetic properties. In addition to these, bismuth oxide glasses are very stable hosts for obtaining efficient luminescence in rare-earth ions. All these applications indicate the need of a basic understanding of the relationship among the electronic polarizability, optical basicity and optical properties of the bismuth oxide glasses.

In this chapter, the synthesis of bismuth oxide and bismuth oxide-doped glasses has been demonstrated. Their physical, optical transmission and basicity, photoluminescence and FTIR reflection properties are examined. Their thermal, electrical and microstructure studies are also reported. In addition, their applications in scientific as well as technological areas are also pointed out.

## 2. EXPERIMENTAL

### 2.1. Synthesis of Bismuth Oxide Glasses

The bismuth glasses are generally synthesized by simple melt quench technique. In this method, batch for glass melting of required size is prepared by using raw materials and are thoroughly mixed for homogeneous mixing in a bowl. After the proper mixing, the mixed batch taken in a suitable crucible such as silica, Alumina, platinum, etc. depending on the melting temperature. For melting of a glass in the range of 800 to 1400<sup>o</sup>C temperature, silica crucible is generally used. But for higher melting temperature (>1400<sup>o</sup>C), platinum crucible is used. The crucible with the batch is then placed in electrically heated furnace and allows the melting for the desired time in which the glass could be melt properly without any un-melted element left behind. For glass melting particularly for bismuth glass, melting temperature and time play a very crucial role. Any variation in these factors could reveal different optical properties. During melting process, intermittent stirring for certain duration is allowed which depend on the size of melt for proper homogeneous mixing. The intermittent stirring is also very important for the removal of curds and bubbles from the glass. After allowing sufficient melting temperature, melting time and intermittent stirring to the melt, the melt is then caste on the graphite mould. The mould should be preheated to the glass transition temperature to avoid any crack for obtain a monolithic glass. The casted glass is then placed in the annealing furnace. The annealing operation is being operated at the  $\pm 10^{\circ}\text{C}$  of glass transition temperature with a suitable programme to release all stress and strain from the glass.

The annealing schedule is again an important factor as it allows slow cooling for the sample to the room temperature.

After proper annealing, now the glass is ready for cutting in different desired size, grinding and polishing for further optical measurement. The grinding and polishing are operated using different size of silicon carbide and cerium oxide powders respectively.

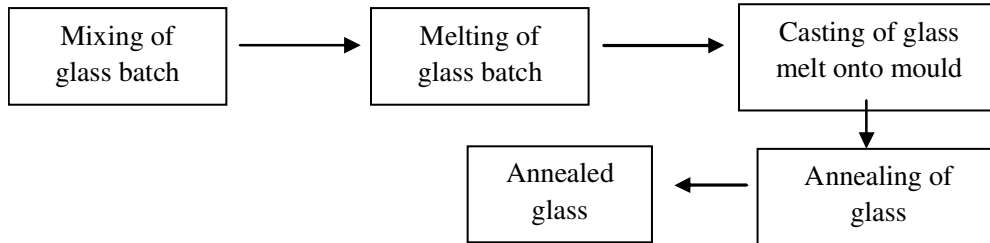


Figure1. Schematic representation of glass preparation.

## 2.2. Synthesis of Bismuth Oxide-Doped Glasses

Bismuth oxide-doped glass samples were also prepared by the conventional melting-quenching technique. Analytical pure reagents of  $\text{Bi}_2\text{O}_3$  along with other glass composition were used as raw materials. The batch mixing, glass melting and annealing process were carried out in the similar way as per the above preparation for the bismuth oxide glasses. The sample preparations by cutting, grinding and polishing for various measurements were also carried out as discussed in the previous section.

## 2.3. Characterization

The softening point ( $T_s$ ) of a glass sample is measured by a glass softening point system (Harrop/Labino, Model SP-3A) with an accuracy of  $\pm 1^\circ\text{C}$ . The instrument is previously calibrated with a NBS (National Bureau of Standards, USA) standard glass of known softening point. The coefficient of thermal expansion (CTE), glass transition temperature ( $T_g$ ) and glass deformation temperature ( $T_d$ ) of the cylindrical shaped glasses are measured with an accuracy of  $\pm 0.2\%$  using a horizontal-loading dilatometer (Netzsch, Model DIL 402 PC) after calibration with a standard alumina supplied with the instrument by the manufacturer. The dielectric constant can be measured with an accuracy of  $\pm 0.5\%$  at a frequency of 1MHz using a LCR meter (Hioki, Model 3532-50 LCR Hitester) at room temperature. Prior to measurement, the instrument first calibrated using Suprasil-W silica glass ( $\epsilon = 3.8$ ). XRD data of glass powder sample are recorded using an XPERTPRO diffractometer (PANalytical) with  $2\theta$  varying from  $10^\circ$  to  $80^\circ$  using Ni filtered  $\text{CuK}\alpha$  ( $\lambda = 1.5406 \text{ \AA}$ ) at  $25^\circ\text{C}$ , generator power of 45 kV and 35 mA. FTIR spectra of polished glass are recorded by a Perkin-Elmer FTIR spectrometer (Model 1600) at a resolution of  $\pm 2 \text{ cm}^{-1}$  after 16 scans. The TEM and SAED images are taken using a FEI instrument (Tehnai-30, ST  $G^2$ ) operating at an accelerating voltage of 200 kV. FESEM photomicrographs are recorded with a Gemini Zeiss Supra<sup>TM</sup> 35VP Model (Carl Zeiss) instrument using an accelerating voltage of 4.9 kV. The sample was prepared for FESEM experiment by etching in 2 wt% of HF solution for 2 minute. The UV-Vis absorption spectra in the range of 200-1100 nm were recorded using 2mm thickness of sample with a double beam UV-visible spectrophotometer (Lambda 20, Perkin-Elmer) at an error of  $\pm 0.1 \text{ nm}$ .

## 3. RESULTS AND DISCUSSION

### 3.1. Bismuth Oxide Glasses

#### 3.1.1. Physical Property

The bismuth oxide contained glasses show higher refractive index. The increase in refractive index is attributed to the generation of non bridging oxygen (NBO) due to incorporation of Bi-O in the glass network. These glasses are also show high density due to the presence of high density bismuth oxides. It is evident that molar volume ( $V_m$ ) of the glasses increase with increase in  $\text{Bi}_2\text{O}_3$  content. The molar volume of the glasses increases due to increase in bond length or inter atomic spacing. It has happened due to the higher ionic radius of  $\text{Bi}^{3+}$  (0.102 nm) than that of other glass former ions. Therefore, it can understand that  $V_m$  as the volume corresponding structural unit with its surrounding space will increase by insertion of bismuth oxide.

#### 3.1.2. Optical Basicity

In the oxide glass, the oxidation state of oxygen is -2. The oxide ion  $\text{O}^{2-}$  is mostly unstable, and so it is not viable to assign a single value for its electronic polarizability. The extent of negative charge borne by oxide (-II) can be expressed by using the optical basicity model, which allows for a simple quantitative relationship between the optical basicity value  $\Lambda$  of an oxide medium and the oxide (-II) polarizability. The optical basicity has been proved also to be a useful parameter for correlating and predicting properties of oxide systems covering a broad range of applications. The average glass basicity, represented by  $\Lambda$  is calculated, from composition by considering the proportion of oxygen (II) atoms contributed by each oxide (this is the equivalent fraction, X), and also taking into account the optical basicity values of individual oxides. The theoretical optical basicity ( $\Lambda_{th}$ ) for the glass in the  $\text{K}_2\text{O}-\text{Bi}_2\text{O}_3-\text{B}_2\text{O}_3$  system has been calculated using the following relation [15, 16].

$$\Lambda_{th} = X(\text{K}_2\text{O}) \Lambda(\text{K}_2\text{O}) + X(\text{Bi}_2\text{O}_3) \Lambda(\text{Bi}_2\text{O}_3) + X(\text{B}_2\text{O}_3) \Lambda(\text{B}_2\text{O}_3) \quad (1)$$

where  $X(\text{K}_2\text{O})$ ,  $X(\text{Bi}_2\text{O}_3)$  and  $X(\text{B}_2\text{O}_3)$  are the equivalent fraction of the different oxides, i.e. the proportion of the oxide atom that contributes to the glass system;  $\Lambda(\text{K}_2\text{O})$ ,  $\Lambda(\text{Bi}_2\text{O}_3)$  and  $\Lambda(\text{B}_2\text{O}_3)$  are the optical basicity values of the constituent oxides. Here the values of  $\Lambda(\text{K}_2\text{O}) = 1.4$ ,  $\Lambda(\text{Bi}_2\text{O}_3) = 1.19$ ,  $\Lambda(\text{B}_2\text{O}_3) = 0.425$  have been taken from the literature [16].

From the above equation, the theoretical optical basicity ( $\Lambda_{th}$ ) values increases with increase in  $\text{Bi}_2\text{O}_3$  content. It is well known that the  $\text{Bi}^{3+}$  cation possesses a very high polarizability ( $1.508\text{\AA}^3$ ), which is due to its large ionic radii and small cationic field strength. In addition,  $\text{Bi}^{3+}$  ions possess a lone pair in the valence shell and therefore, the number of nonbridging oxygen increases with increase in the  $\text{Bi}^{3+}$  ion concentration. Hence it causes an increasing of optical basicity.  $\text{B}_2\text{O}_3$  shows low optical basicity (0.43) and known as strong acidic oxide. But,  $\text{Bi}_2\text{O}_3$  is an oxide with a high basicity (1.19). The increased optical basicity of the glasses with large  $\text{Bi}_2\text{O}_3$  content indicates that the acid-base properties of  $\text{Bi}_2\text{O}_3$  have a significant effect. The low optical basicity is a reduced ability of oxide ions to transfer electrons to the surrounding cations. The borate glasses with a large amount of  $\text{Bi}_2\text{O}_3$  content possess high optical basicity. High optical basicity means high electron donor ability of the oxide ions to the cations. The understanding of optical basicity would be useful for the design of the novel optical functional materials with higher optical performances.

#### 3.1.3. Transmission

The inherent property of bismuth containing glasses is its transparency to near infrared (0.8  $\mu\text{m}$ ) to far infrared region (2.5  $\mu\text{m}$ ). For this reason, the bismuth glasses are very interesting materials for enormous applications in photonics in this region. Generally, the infrared region is very important for communication

purpose. Figure 2 (a and b) show the representative UV-visible and infrared region optical transmission spectra of the glasses in the  $K_2O-Bi_2O_3-B_2O_3$  system.

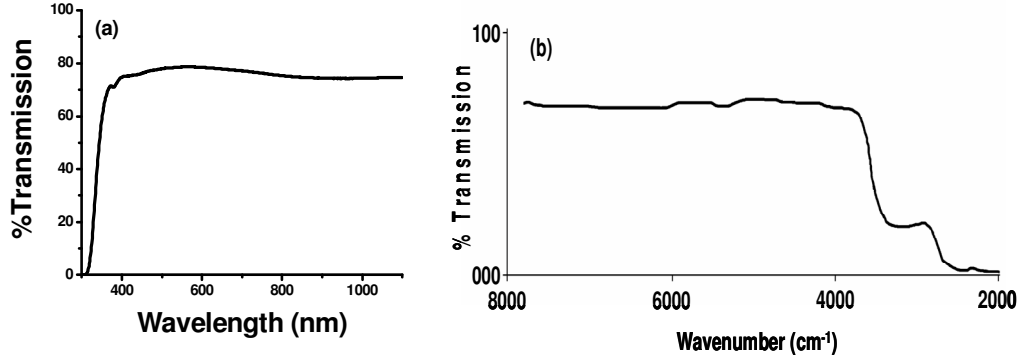


Figure 2. (a) UV-vis and (b) infrared region transmission spectra of a glass in the  $K_2O-Bi_2O_3-B_2O_3$  system.

But, the problem arises in these glasses when they melt at higher temperature and at higher  $Bi_2O_3$  content in the glass. The glasses become brown to black color at higher melting temperature. This blackening is due to the formation of metallic bismuth as a result of auto-thermo reduction during melting. Such glasses show very little transparency.

The absorption spectra of these glasses containing metallic bismuth nanoparticles (NPs) which demonstrated a broad absorption band [17]. This broad absorption is being called as surface plasmon resonance (SPR). The SPR band arises due to the interaction of incoming light with the conduction band electrons of a metal. The SPR absorption band of the glass in the  $K_2O-Bi_2O_3-B_2O_3$  system is shown in the Fig. 3. Figure 3 shows the two SPR bands which arises mainly for two common reasons. First is due to the presence of bimodal size distribution of NPs and secondly the presence of nonspherical NPs. The SPR of a spherical particle gives an absorbance band centered at a wavelength,  $\lambda$ , which can be expressed by the relation [17]

$$\lambda^2 = (2\pi c)^2 m_0 \epsilon_0 (\epsilon_\infty + 2n_0^2) / Ne^2 \quad (2)$$

where  $c$  is the velocity of light,  $m_0$  is the charge carrier mass,  $N$  is the charge carrier particle concentration,  $e$  is the charge of the electron,  $\epsilon_\infty$  is the optical dielectric function of the metal,  $n_0$  is the refractive index (RI) of the host material and  $\epsilon_0$  is the free-space permeability. From the Eq. 1, it is clear that the absorbance band position proportionate directly to the RI of the host material. Because of the interaction of light with the conduction band electron of a metal is different in different refractive index glasses. The absorbance band of  $Bi^0$  NPs in the host water (RI = 1.33) was observed around 400 nm whereas the glass having higher RI (1.76) shows a red shift of the band to 460 nm [17].

The band gap energy of the bismuth glass could be evaluated from the absorption coefficient,  $\alpha$  near the edge of absorption curve. The absorption coefficient,  $\alpha$  was determined by using the following relation [15]

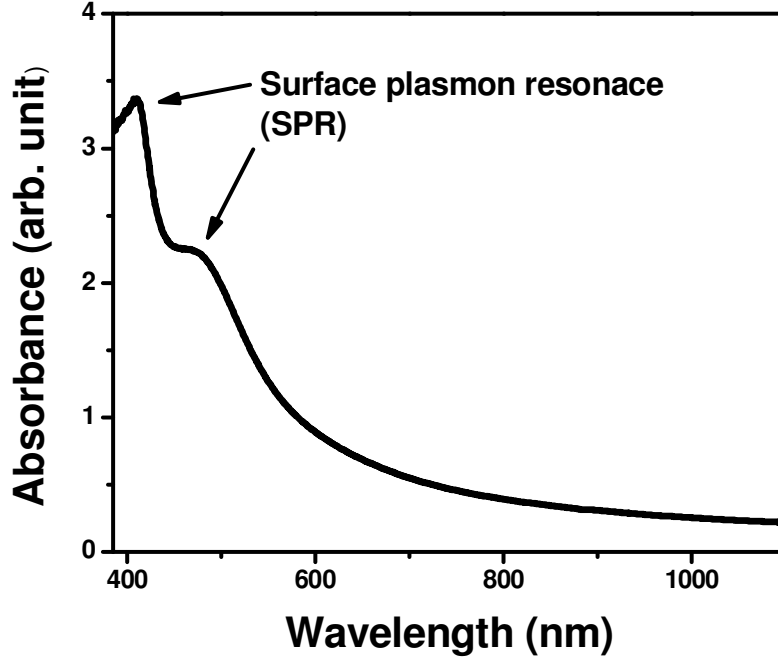


Figure 3. Absorption spectrum of glass in the  $K_2O-Bi_2O_3-B_2O_3$  system.

$$\alpha = 2.303A/t \quad (3)$$

where  $A$  is absorbance and  $t$  is thickness in cm of each sample. The relation between  $\alpha$  and photon energy of the incident radiation,  $h\nu$  is given by the following equation [12].

$$\alpha = B (h\nu - E_{opt})^2 / h\nu \quad (4)$$

where  $B$  is the constant and  $E_{opt}$  is the energy of the optical band gap. The relation (3) can be written as

$$(\alpha h\nu)^{1/2} = B(h\nu - E_{opt}) \quad (5)$$

Using the relation (4) the optical band gap values were determined by the extrapolation of the linear region of the plots of  $(\alpha h\nu)^{1/2}$  vs  $h\nu$ . The value of  $E_{opt}$  obtained is 2.34 eV for the glass in the  $K_2O-Bi_2O_3-B_2O_3$  system using the above equations is shown in Fig. 4. The optical band gap ( $E_{opt}$ ) of the bismuth containing glasses decrease to lower energies with increase in  $Bi_2O_3$  content.

It is related to the progressive increase in the covalent Bi-O of bond strength of  $81.9 \text{ kcal mol}^{-1}$  [13]. Here it is believed that as the cation concentration increases which developed the bridging oxygen bonds with  $Bi^{3+}$  ion and lead to the gradual breakdown of the glass network. This incident seems to account for the decrease in the  $E_{opt}$  value, which results in the shifting of edge to longer wavelength with increase in  $Bi_2O_3$  content. Such a decrease in the values of optical band gap energy can thus be attributed to decrease in the phonon-assistant indirect transitions.

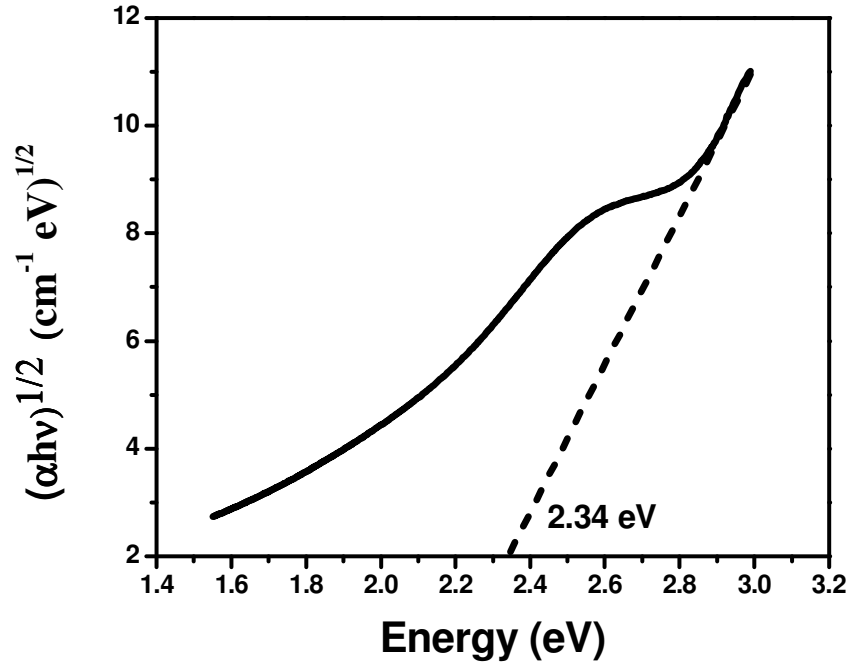


Figure 4. Optical band gap energy of glass in the  $\text{K}_2\text{O-Bi}_2\text{O}_3\text{-B}_2\text{O}_3$  system.

### 3.1.4. Microstructure

In recent years the investigations of bismuth oxide microstructure have been intensified, due to their possible applications in solid oxide fuel cells, oxygen sensors, varistors or electrochromic devices. In bismuth containing glasses, the microstructure observed due to phase separation between the primary phase or bismuth oxide phase and a secondary phase or glassy phase. During melting process, all components are in the liquid phase. Therefore, at the time of quenching process, any of the components get super-saturation state and form a separated secondary phase. This type of phase separation is a very common phenomenon in the glass. Porai-Koshits *et al.* [18], W. Vogel *et al.* [19], James *et al.* [20] and MacDowell *et al.* [21] have worked on the phase separation in various glasses. Porai-Koshits *et al.* [18] have report about such fine structure of sodium silicate glasses arises due to the secondary phase separation from a primary separated phase take place as a result of super saturation under the lowering of temperature during the process of quenching. W. Vogel *et al.* [19] has done electron microscopical studies of phase separated glasses. MacDowell *et al.* [21] has observed metastable glass in glass separation on rapid quenching of  $\text{Al}_2\text{O}_3\text{-SiO}_2$  glass melt. Figure 5 depicts the microstructure of in the  $\text{K}_2\text{O-Bi}_2\text{O}_3\text{-B}_2\text{O}_3$  glass system where secondary phase developed during melting. The micrograph observed by the field emission scanning electron microscopy (FESEM) by performing etching process. The etching is being performed to dissolve the various components present in the glass at various rates using various acids and finally it gives some microstructure. For the glass  $\text{K}_2\text{O-Bi}_2\text{O}_3\text{-B}_2\text{O}_3$  system, the etching process carried out in HF solution, the  $\text{B}_2\text{O}_3$  and  $\text{K}_2\text{O}$  were rapidly dissolved at the time of sample preparation for the FESEM experiment. Therefore the residual  $\text{Bi}_2\text{O}_3$  rich phase could be observed in the micro image as shown in Fig. 5.

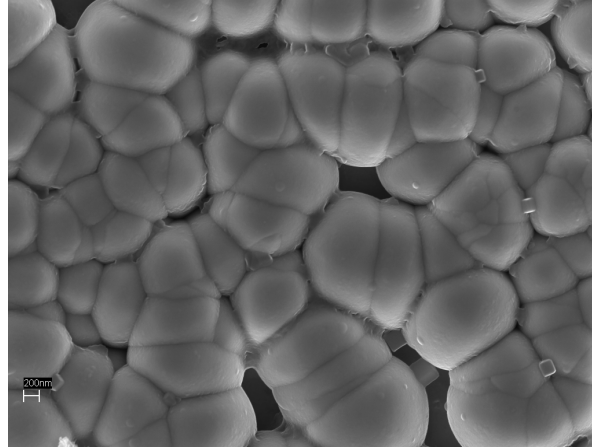


Figure 5. FESEM micrograph of glass in the K<sub>2</sub>O-Bi<sub>2</sub>O<sub>3</sub>-B<sub>2</sub>O<sub>3</sub> system.

### 3.1.5. Transmission electron microscopy

In the previous section it has been discussed that the bismuth glasses lose their transparency at higher melting temperature due to formation of metallic bismuth nanoparticles. The color of the glasses also changes from brown to black with the increase in concentration of Bi<sup>0</sup> NPs. Therefore, the morphology of bismuth nanoparticles revealed spheroidal shape when observed in transmission electron microscopy (TEM). The size of the NPs can be estimated from the TEM image. Figure 6 (A) shows the typical TEM images of Bi<sup>0</sup> NPs in the glass K<sub>2</sub>O-Bi<sub>2</sub>O<sub>3</sub>-B<sub>2</sub>O<sub>3</sub> system. It clearly reveals that the glass has homogeneously dispersed Bi<sup>0</sup> nanoparticles (NPs) of spheroidal shape. The identification of crystalline phase could be analyzed by the selected area electron diffraction (SAED) pattern. Figure 6 (B) demonstrated the selected electron diffraction pattern of rhombohedral crystalline structure of the metallic bismuth.

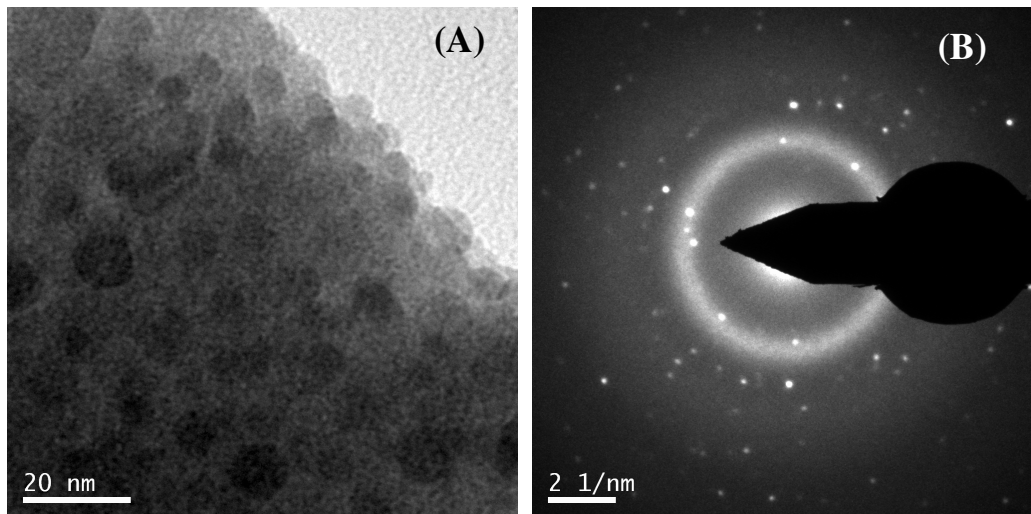


Figure 6. (A) TEM and (B) its SAED images of glass K<sub>2</sub>O-Bi<sub>2</sub>O<sub>3</sub>-B<sub>2</sub>O<sub>3</sub> system.

### 3.1.6. Thermal Properties and Electrical Properties

Thermal property is the important property for the glass. The thermal property of the glass varies with the temperature. During preparation of glass, some thermal properties such as the glass transition temperature, glass softening point temperature and coefficient of thermal expansion are important.

Glass transition temperature ( $T_g$ ) and glass softening point temperature decreases with the increase of  $\text{Bi}_2\text{O}_3$  content in the glass. The content of  $\text{Bi}_2\text{O}_3$  increases into the glass systems which results in splitting of glass network former bonds and hence the bridging oxygens (BOs) are converted into non bridging oxygens (NBOs). Further addition of  $\text{Bi}_2\text{O}_3$  into glass opens up the glass network. This results in weakening of the glass structure. Hence the glass transition temperature and glass softening point temperature decrease with the increase in  $\text{Bi}_2\text{O}_3$  content. It is obvious that the decreases in the above values are due to increase in the number of Bi-O which is weaker than that of glass former bond strength. Figure 7 shows the glass transition temperature ( $T_g$ ) evaluated by dilatometer for the glass in the  $\text{K}_2\text{O}-\text{Bi}_2\text{O}_3-\text{B}_2\text{O}_3$  system.

The thermal expansion of glasses is controlled by the asymmetry of the amplitude of thermal vibrations in the glass. It decreases as the rigidity of the glass network increases [22]. An increase of the number of non-bridging bonds weakens the structure which in turn increases the coefficient of thermal expansion. Here, the coefficient of thermal expansion measured in the range of  $300-350^\circ\text{C}$ , and it gradually decreases with the increase in the  $\text{Bi}_2\text{O}_3$  content in the glasses which is shown in the Fig. 7.

The dielectric constant is directly correlated with the polarizability of the glass. The dielectric constant gradually increases with the increase in the  $\text{Bi}_2\text{O}_3$  content in the glasses. It has already been reported that  $\text{Bi}^{3+}$  ions are highly polarizable (above  $3 \text{ \AA}^3$ ) due to their large ionic radii and small cation unit field strength [5, 13].

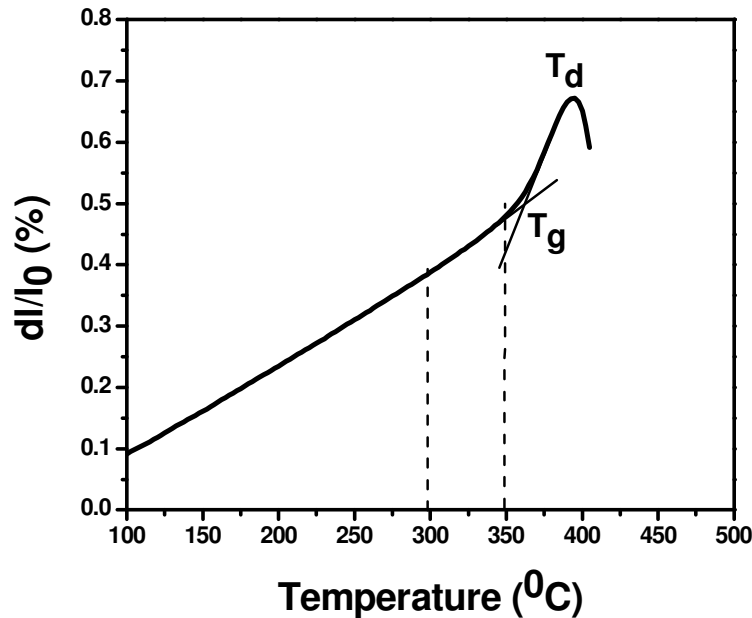
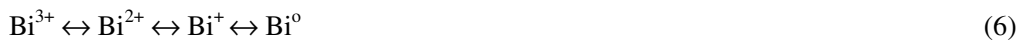


Figure 7. Co-efficient of thermal expansion (CTE) spectra of glass in the  $\text{K}_2\text{O}-\text{Bi}_2\text{O}_3-\text{B}_2\text{O}_3$  system.

### 3.1.7. Photoluminescence

In recent time, bismuth glasses have attracted attention of various researchers as a very important optical material from the view point of its photoluminescence properties for photonics and optoelectronic applications. Bismuth has several kinds of valence states simultaneously existing in glasses. The various emission centers in the bismuth glass causes due to various ionic species of bismuth (e.g.,  $\text{Bi}^{5+}$ ,  $\text{Bi}^{3+}$ ,  $\text{Bi}^{2+}$  and  $\text{Bi}^+$ ) [23-29]. The formation of various valence state of bismuth take place by the auto-thermo reduction of  $\text{Bi}^{3+}$  ions proceeds towards  $\text{Bi}^0$  reversibly during melting process through the following intermediate valence states:



It is not clear that which valence of bismuth ion contributes to the various emissions up to now. The blue to green region emission has been reported by  $\text{Bi}^{3+}$  ions where as the red emission due to  $\text{Bi}^{2+}$  ionic species. The bismuth glasses show very interesting NIR emissions which are very important from the point view of optical communication. The emission center in NIR region is not clearly understood still now. Some researchers have reported the NIR emission due to  $\text{Bi}^+$  and some are reported as  $\text{Bi}^{5+}$ . The metallic bismuth ( $\text{Bi}^0$ ) NPs is also causes NIR emission and has been demonstrated by various researchers. The energy diagram of various energy levels is shown in Fig. 8.

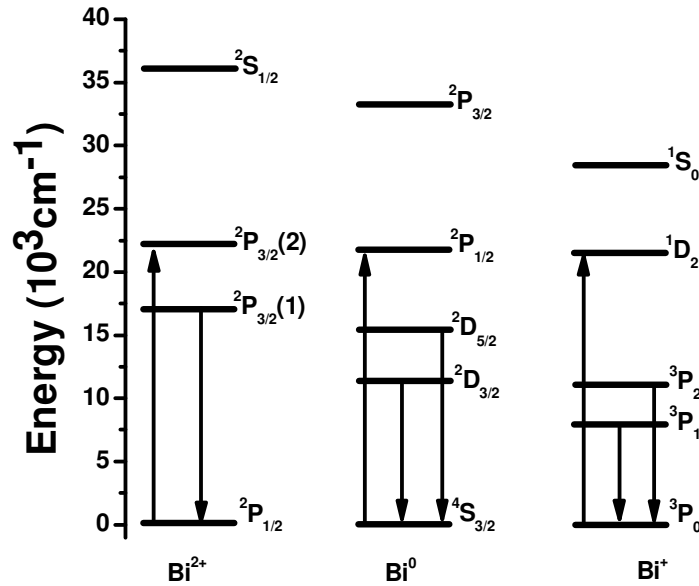


Figure 8. Schematic energy level diagrams for  $\text{Bi}^{2+}$ ,  $\text{Bi}^+$  and  $\text{Bi}^0$  centers.

### 3.1.8. Fourier Transformation Infrared Reflectance Spectroscopy (FTIRRS)

$\text{Bi}_2\text{O}_3$  containing glasses have fundamental vibrations in the IR spectral regions at around  $480$  and  $715\text{ cm}^{-1}$  [30, 31]. In Fig. 9 shows Fourier transformation infrared reflectance spectroscopy (FTIRRS) of glass in the  $\text{K}_2\text{O-Bi}_2\text{O}_3\text{-B}_2\text{O}_3$  system. The reflection bands at  $451\text{ cm}^{-1}$ , specific to the vibrations of Bi–O bonds in  $\text{BiO}_6$  octahedral units [30, 31]. The absorption band at  $707\text{ cm}^{-1}$  has been assigned to symmetric stretching vibrations of Bi–O bonds in  $\text{BiO}_3$  pyramidal units [30, 31]. The band at  $882\text{ cm}^{-1}$  is due to stretching vibration of the B–O bonds in tetrahedral  $\text{BO}_4$  unit and the broad band at  $1180$  and  $1265\text{ cm}^{-1}$  is attributed to the B–O bond stretching in the planar  $\text{BO}_3$  unit in the borate network [30-35].

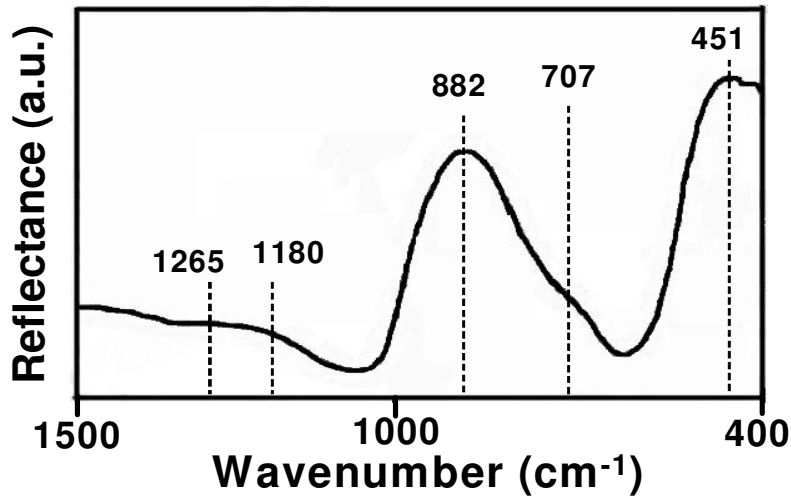


Figure 9. FTIR spectrum of glass in the K<sub>2</sub>O-Bi<sub>2</sub>O<sub>3</sub>-B<sub>2</sub>O<sub>3</sub> system.

### 3.2. Bismuth Oxide-Doped Glasses

In recent years, subsequent research on bismuth oxide-doped glasses for their near infrared (NIR) photoluminescence (PL) has been developed in different host materials such as silicate [23–25], germanate [26, 27], phosphate and barium borate [2], etc. The most interesting property of Bi<sub>2</sub>O<sub>3</sub>-doped glasses is their emission having large width, which placed them distinctly from traditional rare earth dopants such as erbium and neodymium. In all type of host glasses, the reported luminescences is centered at around 1.2 μm and present a full width at half maximum from 200 to 400 nm approximately. However, the luminescent center responsible for this PL is not clearly known till now. Different reports attributed the origin of this NIR PL to the electronic transition of Bi<sup>5+</sup>, Bi<sup>+</sup>, Bi<sup>2+</sup>, Bi<sup>0</sup>, or to BiO molecules in the glass host [23–29]. Truong *et al.* [36] have studied about the thermal stability of Bi-doped silicate fibers and their corresponding performs. They concentrated on the results of the NIR emission quenching properties in the case of hydrogen-loaded and annealed fibers. Seo *et al.* [37] have been developing a new laser medium based on silica glass and have discovered a new infrared emission from a bismuth-doped silica glass. They also achieved an optical amplification in a bismuth-doped silica fiber at 1308 nm with an 810- nm excitation. Zhou *et al.* [1] have demonstrated the ultra-broadband luminescent sources that emit light over an extremely wide wavelength range which are of great interest in the fields of photonics, medical treatment, and precision measurement. They present a simplistic method to realize this kind of novel light source by stabilizing bismuth active centers in a nanoporous silica glass. The obtained highly transparent materials, in which multiple bismuth centers such as Bi<sup>+</sup>, Bi<sup>2+</sup>, and Bi<sup>3+</sup> have stabilized. It emit in an ultra-broadband wavelength range from blue-green, orange, red, and white to the near-infrared region. This tunable luminescence covers the spectral range of the three primary colors (red, green and blue) and also the telecommunications windows.

The worldwide decrease in the fossil fuel reserve is the future concern of energy supply has been widely attracted the attention of many researchers towards the development of an alternative energy sources. Photovoltaic energy conversion is one of the most widely accepted alternatives for future energy crisis solution. The photovoltaic cell is based on the unlimited supply of sunlight and the photoelectric properties of silicon. It has been the subject of extensive research efforts for many decades. The sunlight to electricity conversion efficiency of silicon-based solar cells has now reached more than 22 % [38]. Their spectral sensitivity to incoming light is broadly distributed over the visible (VIS) to near infrared (NIR) spectral range. The silicon-based solar cells exhibit the band gap energy of 1.12 eV. It indicates that the light of a wavelength

longer than 1100 nm can not be converted into electricity. In the past, to improve the spectral overlap between cell sensitivity and incoming light, both up and down conversion of parts of the solar spectrum have been considered [39, 40]. From the view point of cell design, down-conversion is important for incoming light incident on the cover plate of the solar cell. The incident light is partly converted to higher wavelengths and partly transmitted. Efficiency is determined by the transparency of the material at wavelengths that lie above the luminescence excitation bands must not be lost by any other absorption. In up-conversion designs, the opposite event has been observed. Here, high transmission cover plate materials would be required at wavelengths below the excitation band for up-conversion. This is usually not happened. Therefore, the up-conversion designs rely on backside coatings. The converter material is placed on the backside of the cell material and only light that has passed the solar cell is converted. In this context, only down-conversion materials show promise as luminescent concentrators (LC) [40]. Here the light that falls on a converter plate is first converted and subsequently, transported to the edges of the plate by total reflection. Through luminescence, light is concentrated on the edges which are covered with the cell material. LC materials that are suitable to improve photovoltaic cell efficiency by down-conversion are still rare. The desired parameter for the potential LC materials is its strong excitation bands in the UV-VIS and high quantum efficiency of VIS-NIR emission. In this context, Peng *et al.* [41] have demonstrated the various glasses doped with up to 2 mol% of  $\text{Bi}_2\text{O}_3$ , which are also considered as potential LC materials that meet the above requirements. They established how their luminescence properties offer a unique alternative for planar solar converters and concentrators for more efficient photo and photo thermo voltaic (PTV) cells.

#### 4. APPLICATIONS

It has been known that the synthesis of heavy metal oxide (HMO) glasses is important due to their high refractive index, low phonon energy and high density [9, 10]. Bismuth based HMO glasses exhibit large third-order nonlinear optical susceptibility and are important candidates for optic and optoelectronic components [42, 43]. These glasses are transparent material which is thermally and chemically stable; therefore, it is a promising dielectric medium for encapsulation of various nanometals. Again these glasses are itself a very elegant material for technology as well as academic point of view due to their inherent superiority over other dielectric. So the study of nanometal embeded bismuth glass nanocomposites is a very important and interesting subject and need to explore its novel preparative methods and properties. The synthesis of nanoparticles of various metals such as silver, gold, platinum etc. in the bismuth glass could enhance its photoluminescence as well as non linear properties to a large extent. But, it is very difficult to synthesize the nanometal embedded bismuth glass nanocomposites as bismuth has tendency to reduce itself to metallic bismuth by auto-thermo reduction at high melting temperature. It is known that glasses embedded with metal nanoparticles may exhibit different colors, depending on whether they are viewed in transmission or reflection lights. This phenomenon termed as dichroic which exhibits different colors at different angles [44, 45]. These dichroic glasses have enormous application in the field of dichroic polarizer, coating, sensor etc.

The study of the nanoparticles (NPs) is the emerging field which has enormous potential for advanced research in twenty first century. The electrons of conduction band of the nanoparticle interact with the various forms of energy (i.e. light, electrical, magnetic, etc.) show very interesting results which are not shown by its bulk form. When electromagnetic radiation of particular wavelength interacts with a nanoparticle to create a coherent oscillation of the conduction band electrons termed as a surface plasmon resonance (SPR) of the NP [46-50]. The study of surface plasmon of the noble metal nanoparticles has been fascinated interests of a various researchers for their various applications such as waveguide, photonics circuits, sensors, etc [44, 51-59]. All of these applications are based on the local field effect (LFE) of surface plasmon resonance of the nanoparticles which has emerged into a new area of nanophotonics called plasmonics. The SPR band strongly depends on the shape, size, distribution and concentration of the metal clusters. Any techniques allowing

manipulation of the above mentioned parameters of such nanocomposite materials in a controlled way are very promising in view of their applications in the field of nanophotonics; this includes manufacturing of nonlinear materials, nanodevices, optical elements, etc. The observation of multiple plasmon peaks is another feature of interest for the localized surface plasmon resonance (LSPR) spectra of spherical, nanorods, triangular nanoprisms, hexagonal and nanocubes [46-50]. These are developed either by multipolar excitation or by interaction with the environment, such as with an asymmetric dielectric environment or with other nearby metal particles. In our work [60], we demonstrated a novel one-step melt quench synthesis method of the bismuth coated spherical and hexagonal silver nanoparticles in the bismuth glass nanocomposites. Here we have shown the alteration of the SPR bands by changing the shape and sizes of bismuth coated silver nanoparticles with the gradual incorporation of silver nanoparticles as well as the thermal treatment duration on the bismuth glass nanocomposites. The change in absorption spectra of lower and higher concentration of silver has been shown in the Fig. 10.

Bismuth glasses show various emission centers from the ultraviolet-Visible-infrared region for presence of various species of bismuth such as  $\text{Bi}^{3+}$ ,  $\text{Bi}^{2+}$ ,  $\text{Bi}^+$ ,  $\text{Bi}^0$ , etc. [2, 23-29]. Therefore these glasses are very promising optical materials for photonic as well as optoelectronic applications. The rare earth doped bismuth glasses show enhanced photoluminescence. These enhanced photoluminescence observed due to energy transfer mechanism from the above ionic species of bismuth. These rare earth doped bismuth glasses are therefore promising materials to obtained high efficient emissions from various rare earth ions.

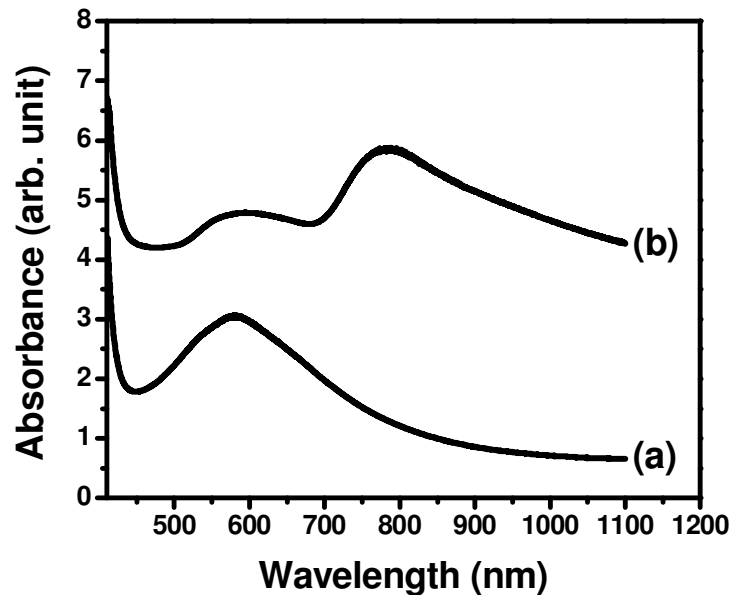


Figure 10. Alteration of surface plasmon resonance bands of silver nanoparticles at (a) lower and (b) higher concentration in bismuth glass nanocomposites.

$\text{Bi}_2\text{O}_3$ -containing glasses exhibit extremely large third-order nonlinear optical susceptibilities and are excellent host materials for rare-earth doping to get efficient fluorescence emissions because of their low phonon energies [61, 62]. On the other hand, optically transparent crystallized glasses containing rare-earth ions or ferroelectric crystals have received much interest, because such materials have high potential for laser host, tunable waveguide, tunable fiber grating, and so on. It is of interest to fabricate transparent  $\text{Bi}_2\text{O}_3$ -based crystallized glasses showing optical nonlinearities or containing rare-earth ions.

Refractive index is the most significant optical property of glass, because this index shows interaction between light and glass material. High refractive index enhances or affects emission property or optical non-linearity. Thus this feature is very important for the advanced optical telecommunication and processing

devices in both wavelength division multiplexing (WDM) and optical time division multiplexing (OTDM) systems. Heavy metal oxide glasses containing  $\text{TeO}_2$ ,  $\text{PbO}$ ,  $\text{Ga}_2\text{O}_3$  and  $\text{Bi}_2\text{O}_3$  are well known to show high refractive index. However, glasses which exhibit refractive index higher than 2.0 with higher thermal stability for fiber drawing are not practically available. In this context the bismuth oxide based glasses, which could show refractive indices higher than 2.0 with higher thermal stability, and have fabricated optical fiber using these glasses for erbium doped fiber amplifier (EDFA) and non-linear applications [63].

Bismuth, a semimetal with a rhombohedral structure, possesses many useful properties such as it has a small energy overlap between the conduction and valence bands, high carrier motilities, and highly anisotropic Fermi surface that make it attractive for different applications [64-66]. Small effective mass makes bismuth nanoparticles an interesting scheme for studying quantum confinement effects [67, 68]. Recent work also has suggested that Bi materials of reduced dimensions may exhibit enhanced thermoelectric properties at room temperature [66]. Various researchers have carried out different experiments on the change of morphology of bismuth nanoparticles under the electron beam irradiation in TEM [69-71]. The electron beam irradiation exhibited rhombohedral structure of bismuth nanoparticles. The bismuth glass dielectric is itself a very fascinating material from the point of view of various technological applications. Therefore, how the effect of electron beam irradiation is used to good advantage to the formation of bismuth nanocrystals in bismuth glass dielectrics is again a very attractive methodology. The formation of bismuth nanocrystals by electron beam irradiation is very important tool for nanolithography and nanopatterning in optoelectronics applications due to rapid formation of bismuth nanocrystal in bismuth glass dielectrics.

## 5. CONCLUSION

There is a renewed interest in the bismuth and bismuth doped glasses due to their inherent superior character over other type of glasses. Bismuth glass is one of the most important amongst the heavy metal oxide (HMO) glasses. The glasses are characterized by low melting temperature, high density, high refractive index, high coefficient of thermal expansion, high dielectric constant, low softening point, wide transmission window, broad band near infrared (NIR) emission, etc. Beside these properties, bismuth glasses are also new promising substitute for the lead base glasses. These facts make bismuth glasses a very attractive eco friendly material for various applications such as in plasma display panels, glass sealing, radiation shielding glass, etc.

Bismuth oxide ( $\text{Bi}_2\text{O}_3$ ) based glasses for their high polarizability has fascinated much attention of glass researchers because of their nonlinear optical properties which have importance for the development of optical information processing technology. Therefore, many studies on their structure and optical properties have been carried out. These glasses are also a very important optical material from the view point of its photoluminescence properties. The glasses are very stable hosts for obtaining efficient luminescence in rare-earth ions. Recently synthesis of bismuth nanoparticles (NPs) in various dielectric host materials has fascinated some researchers for their plasmonics study and it could enable many new applications. But the synthesis of Bi NPs in glass dielectric has not been studied extensively. The noble metal such as Ag has strong localized surface plasmon resonance (LSPR) effects. Therefore, the presence of these novel metals in such highly infrared transmitted bismuth glass could explore some new applications in the field of photonics and optoelectronic. The rapid formation of bismuth nanocrystal under electron beam irradiation is very useful tool for nanopatterning and nanolithography applications. Bismuth oxide-doped glasses have also enormous applications in the field of photonics as well as optoelectronics.

## ACKNOWLEDGEMENTS

SPS express his sincere gratitude for the financial support of the Council of Scientific and Industrial Research (CSIR), New Delhi in the form of CSIR-SRF under the sanction number 31/15(78)/2010-EMR-I. The authors thank Director of the institute for his kind permission to publish this article. They also thankfully acknowledge the Electron Microscope Division of this institute for recording the FESEM, TEM, and SAED images.

## REFERENCES

- [1] Zhou, S., Jiang, N., Zhu, B., Yang, H., Ye, S., Lakshminarayana, G., Hao, J., & Qiu, J. (2008). *Multifunctional Bismuth-Doped Nanoporous Silica Glass: From Blue-Green, Orange, Red, and White Light Sources to Ultra-Broadband Infrared Amplifiers*. *Adv. Funct. Mater.*, 18, 1407-1413.
- [2] Meng, X., Qiu, J., Peng, M., Chen, D., Zhao, Q., Jiang, X., & Zhu, C. (2005). *Near Infrared Broadband Emission of Bismuth-Doped Aluminophosphate Glass*. *Optics Exp.*, 13, 1628-1634.
- [3] Wang, Y., Dai, S., Chen, F., Xu, T., & Nie, Q. (2009). *Physical Properties and Optical Band Gap of New Tellurite Glasses within the  $TeO_2$ - $Nb_2O_5$ - $Bi_2O_3$  System*. *Mater. Chem. Phys.*, 113, 407-411.
- [4] Opera, I., Hesse, H., & Betzler, K. (2004). *Optical Properties of Bismuth Borate Glasses*. *Opt. Mater.* 26, 235-237.
- [5] Zhao, X., Wang, X., Lin, H., & Wang, Z. (2007). *Correlation among Electronic Polarizability, Optical Basicity and Interaction Parameter of  $Bi_2O_3$ - $B_2O_3$  Glasses*. *Physica B*, 390, 293-300.
- [6] Łączka, M., Stoch, L., & Górecki, J. (1992). *Bismuth-containing glasses as materials for optoelectronics*. *J. Alloys Compd.*, 186, 279-291.
- [7] An, J-S., Park, J-S., Kim, J-R., & Hong, K. S. (2006). *Effects of  $Bi_2O_3$  and  $Na_2O$  on the Thermal and Dielectric Properties of Zinc Borosilicate Glass for Plasma Display Panels*. *J. Am. Ceram. Soc.*, 89, 3658-3661.
- [8] Hrovat, M., Maeder, T., Holc, J., Belavič, D., Cilenšek, J., & Bernard, J. (2008). *Subsolidus Phase Equilibria in the  $RuO_2$ - $Bi_2O_3$ - $SiO_2$  System*. *J. Euro. Ceram. Soc.*, 28, 2221-2224.
- [9] Sanz, O., Haro-Poniatowski, E., Gonzalo, J., & Fernández Navarro, J. M. (2006). *Influence of the Melting Conditions of Heavy Metal Oxide Glasses Containing Bismuth Oxide on their Optical Absorption*. *J. Non-Cryst. Solids*, 352, 761-768.
- [10] Zhang, Y., Yang, Y., Zheng, J., Hua, W., & Chen, G. (2008). *Effects of Oxidizing Additives on Optical Properties of  $Bi_2O_3$ - $B_2O_3$ - $SiO_2$  Glasses*. *J. Am. Ceram. Soc.* 91, 3410-3412.
- [11] Sun, H., Wen, L., Xu, S., Dai, S., Hu, L., & Jiang, Z. (2005). *Novel Lithium-Barium-Lead-Bismuth Glasses*. *Mater. Lett.*, 59, 959-962.
- [12] Lee, S., Hwang, S., Cha, M., Shin, H., & Kim, H. (2008). *Role of Copper Ion in Preventing Silver Nanoparticles Forming in  $Bi_2O_3$ - $B_2O_3$ - $ZnO$  Glass*. *J. Phys. Chem. Solids*, 69, 1498-1500.
- [13] Saritha, D., Markandeya, Y., Salagram, M., Vithal, M., Singh, A. K., & Bhikshamaiah, G. (2008). *Effect of  $Bi_2O_3$  on Physical, Optical and Structural Studies of  $ZnO$ - $Bi_2O_3$ - $B_2O_3$  Glasses*. *J. Non-Cryst. Solids*, 354, 5573-5579.
- [14] Qiu, H. H., Ito, T., & Sakata, H. (1999). *DC Conductivity of  $Fe_2O_3$ - $Bi_2O_3$ - $B_2O_3$  Glasses*. *Mater. Chem. Phys.*, 58, 243-248.
- [15] Dimitrov, V., & Komatsu, T. (2005). *Classification of Oxide Glasses: A Polarizability Approach*. *J. Solid State Chem.*, 178, 831-846.
- [16] Duffy, J. A., Ingram, M. D. (1991). *Optical Properties of Glass*. (pp. 159-184) Westerville: The American Ceramic Society.

- [17] Singh, S. P., & Karmakar, B. (2010). *Oxidative Control of Surface Plasmon Resonance of Bismuth Nanometal in Bismuth Glass Nanocomposites*. Mater. Chem. Phys., 119, 355-358.
- [18] Porai-Koshits, E. A., & Averjanov, V. I. (1968). *Primary and Secondary Phase Separation of Sodium Silicate Glasses*. J. Non-Cryst. Solids, 1, 29-38.
- [19] Vogel, W., Horn, L., Reiss, H., & Volksch, G. (1982). *Electron-Microscopical Studies of Glass*. J. Non-Cryst. Solids, 49, 221-240.
- [20] James, P. F., & McMillan, P. W. (1970). *Quantitative Measurements of Phase Separation in Glasses using Transmission Electron Microscopy-1. Experimental Technique and Method of Analysis*. Phys. Chem. Glasses, 11 ( 3), 59-70.
- [21] MacDowell, J. F., Beall, G. H. (1969). *Immiscibility and Crystallization in  $Al_2O_3$ - $SiO_2$  Glasses*. J. Am. Ceram. Soc., 52 ( 1), 37-45.
- [22] Gavriiliu, G. (2002). *Thermal Expansion and Characteristic Points of  $-Na_2O$ - $SiO_2$  Glass with added Oxides*. J. Euro. Ceram. Soc., 22, 1375-1379.
- [23] Peng, M., Chen, D., Qiu, J., Jiang, X., & Zhu, C. (2007). *Bismuth-Doped Zinc Aluminosilicate Glasses and Glass-Ceramics with Ultra-Broadband Infrared Luminescence*. Opt. Mater., 29, 556-561.
- [24] Fujimoto, Y., & Nakatsuka, M. (2003). *Optical Amplification in Bismuth-Doped Silica Glass*. Appl. Phys. Lett., 82, 3325-1-2.
- [25] Arai, Y., Suzuki, T., Ohishi, Y., Morimoto, S., & Khonthon, S. (2007). *Ultrabroadband Near-Infrared Emission from a Colorless Bismuth-Doped Glass*. Appl. Phys. Lett. 90, 261110-1-3.
- [26] Xia, H. P., & Wang, X. J. (2006). *Near Infrared Broadband Emission from  $Bi^{5+}$ -Doped  $Al_2O_3$ - $GeO_2$ - $X$  ( $X=Na_2O, BaO, Y_2O_3$ ) Glasses*. Appl. Phys. Lett. 89, 051917.
- [27] Peng, M., Qiu, J., Chen, D., Meng, X., Yang, I., Jiang, X., & Zhu, C. (2004). *Bismuth and Aluminum-Codoped Germanium Oxide Glasses for Super-Broadband Optical Amplification*. Opt. Lett. 29, 1998-2000.
- [28] Singh, S. P., Chakradhar, R. P. S., Rao, J. L., & Karmakar, B. 2010. *EPR, FTIR, Optical Absorption and Photoluminescence Studies of  $Fe_2O_3$  and  $CeO_2$  Doped  $ZnO$ - $Bi_2O_3$ - $B_2O_3$  Glasses*. J. Alloys Compd., 493, 256-262.
- [29] Singh, S. P., Chakradhar, R. P. S., Rao, J. L., & Karmakar, B. (2010). *EPR, Optical Absorption and Photoluminescence Properties of  $MnO_2$  Doped  $23B_2O_3$ - $5ZnO$ - $72Bi_2O_3$  Glasses*. Physica B, 405, 2157-2161.
- [30] Doweidar, H., & Saddeek, Y. B. (2009). *FTIR and Ultrasonic Investigations on Modified Bismuth Borate Glasses*. J. Non-Cryst. Solids, 355, 348-354.
- [31] Ardelean, I., Cora, S., Rusu, D. (2008). *EPR and FT-IR Spectroscopic Studies of  $Bi_2O_3$ - $B_2O_3$ - $CuO$  Glasses*. Physica B, 403, 3682-3685.
- [32] Fuxi, G. (1992). *Optical and Spectroscopic properties of Glass*. Berlin: Springer-Verlag.
- [33] Kamitsos, E. I., Karakassides, M. A., & Chryssikos, G. D. (1987). *Vibrational Spectra of Magnesium-Sodium-Borate Glasses. 2. Raman and Mid-Infrared Investigation of the Network Structure*. J. Phys. Chem. 91 (5), 1073-1079.
- [34] Kharlamov, A. A., Almeida, R. M., & Heo, J. (1996). *Vibrational Spectra and Structure of Heavy Metal Oxide Glasses*. J. Non-Cryst. Solids, 202, 233-240.
- [35] Motke, S. G., Yowale, S. P., & Yawale, S. S. (2002). *Infrared Spectra of Zinc Doped Lead Borate Glasses*. Bull. Mater. Sci., 25, 75-78.
- [36] Truong, V. G., Bigot, L., Lerouge, A., Douay, M., & Razdobreev, I. (2008). *Study of Thermal Stability and Luminescence Quenching Properties of Bismuth-Doped Silicate Glasses for Fiber Laser Applications*. Appl. Phys. Lett., 92, 041908-1-3.
- [37] Seo, Y. S., Lim, C., Fujimoto, Y., Nakatsuka, M., (2007). *Bismuth-Doped Silica Glass as a New Laser Material*. J. Kor. Phys. Soc., 51, 364-367.
- [38] Green, M. A. (1987). *High Efficiency Silicon Solar Cells*. Aedermannsdorf: Trans. Tech.

- [39] van Sark, W., Meijerink, A., Schropp, R., van Roosmalen, J., Lysen, E. (2005). *Enhancing Solar Cell Efficiency by Using Spectral Converters*. Solar Energ. Mat. Sol. C, 87, 395-409.
- [40] Weber, W., & Lambe, J. (1976). *Luminescent Greenhouse Collector for Solar Radiation*. Appl. Optics, 15, 2299-2300.
- [41] Peng, M., & Wondraczek, L., (2009). *Bismuth-Doped Oxide Glasses as Potential Solar Spectral Converters and Concentrators*. J. Mater. Chem., 19, 627-630.
- [42] Deparis, O., Mezzapesa, F. P., Corbari, C., Kazansky, P. G., & Sakaguchi, K. (2005). *Origin and Enhancement of the Second-Order Non-Linear Optical Susceptibility Induced in Bismuth Borate Glasses by Thermal Poling*. J. Non-Cryst. Solids, 351, 2166-2177.
- [43] Kustov, E. F., Bulatov, L. I., Dvoyrin, V.V., & Mashinsky, V. M. (2009). *Molecular Orbital Model of Optical Centers in Bismuth-Doped Glasses*. Optics Lett., 34, 1549-1551.
- [44] Magruder III, R. H., Robinson, S. J., Smith, C., Meldrum, A., Halabica, A., & Haglund Jr, R. F. (2009). *Dichroism in Ag Nanoparticle Composites with Bimodal Size Distribution*. J. Appl. Phys. 105, 024303-1-5.
- [45] Cortie, M. B., Xu, X. & Ford, M. J. (2006). *Effect of Composition and Packing Configuration on the Dichroic Optical Properties of Coinage Metal Nanorods*. Phys. Chem. Chem. Phys. 8, 3520-3527.
- [46] Bréchnignac, C., Houdy, P., & Lahmani, M. (2007). *Nanomaterials and Nanochemistry*. Berlin: Springer.
- [47] Ferrando, R., Jellinek, J., & Johnston, R. L. (2008). *Nanoalloys: From Theory to Applications of Alloy Clusters and Nanoparticles*. Chem. Reviews, 108, 845-910.
- [48] Schiffrin, D. J. (2004). *Faraday Discussions: Nanoparticle Assemblies*. (Vol. 125) Cambridge: RSC.
- [49] Rao, C. N. R., Müller, A., Cheetham, A. K. (2004). *The Chemistry of Nanometals: Synthesis, Properties and Applications*. (Vol. 2) Weinheim: Wiley-Vch.
- [50] Corain, B., Schmid, G., & Toshima, N. (2008). *Metal Nanoclusters in Catalysis and Materials Science: The Issue of Size Control*. Amsterdam: Elsevier.
- [51] Houk, R. J. T., Jacobs, B. W., Gabaly, F. E. I., Chang, N. N., Talin, A. A., Graham, D. D., House, S. D., Robertson, I. M., & Allendorf, M. D. (2009). *Silver Cluster Formation, Dynamics, and Chemistry in Metal–Organic Frameworks*. Nano Lett., 9, 3413-3418.
- [52] Sherry, L. J., Jin, R., Mirkin, C. A., Schatz, G. C., & Duynes, R. P. V. (2006). *Localized Surface Plasmon Resonance Spectroscopy of Single Silver Triangular Nanoprisms*. Nano Lett., 6, 2060-2065.
- [53] Choi, B-h., Lee, H-H., Jin, S., Chun, S., & Kim, S-H. (2007). *Characterization of the Optical Properties of Silver Nanoparticle Films*. Nanotechnology, 18, 075706-1-5.
- [54] Konta, R., Kato, H., Kobayashi, H., & Kudo, A. (2003). *Photophysical Properties and Photocatalytic Activities under Visible Light Irradiation of Silver Vanadates*. Phys. Chem. Chem. Phys., 5, 3061-3065.
- [55] Huxter, V. M., & Scholes, G. D. (2009). *Photophysics of Colloidal Semiconductor Nanocrystals: a Review*. J. Nanophotonics, 3, 032504-1-15.
- [56] Bhattacharyya, S., Bocker, C., Heil, T., Jinschek, J. R., Höche, T., Rüssel, C., Kohl, H. (2009). *Experimental Evidence of Self-Limited Growth of Nanocrystals in Glass*. Nano. Lett., 9, 2493-2496.
- [57] Benahmed, A. J., & Ho, C. M. (2007). *Bandgap-Assisted Surface-Plasmon Sensing*. Appl. Optics, 46, 3369-3375.
- [58] Okamoto, T., H'Dhili, F., & Kawata, S. (2004). *Towards Plasmonic Band Gap Laser*. Appl. Phys. Lett., 85, 3968-1-3.
- [59] Scalora, M., Bloemer, M. J., Pethel, A. S., Dowling, J. P., Bowden, C. M., & Manka, A. S. 1998. *Transparent, Metallo-Dielectric, One-Dimensional, Photonic Band-Gap Structures*. J. Appl. Phys., 83, 2377-1-7.
- [60] Singh, S. P., & Karmakar, B. (2011). *Single-Step Synthesis and Surface Plasmons of Bismuth-Coated Spherical to Hexagonal Silver Nanoparticles in Dichroic Ag:Bismuth Glass Nanocomposites*. Plasmonics, DOI 10.1007/s11468-011-9224-5, (in press).

- [61] Nasu, H., Ito, T., Hase, H., Matsuoka, J., & Kamiya, K. (1996). *Third-Order Optical Non-Linearity of Bi<sub>2</sub>O<sub>3</sub>-Based Glasses*. J. Non-Cryst. Solids, 204, 78-82.
- [62] Tanabe, S., Hirao, K., & Soga, N. (1990). *Upconversion Fluorescences of TeO<sub>2</sub>- and Ga<sub>2</sub>O<sub>3</sub>-Based Oxide Glasses Containing Er<sup>3+</sup>*. J. Non-Cryst. Solids, 122, 79-82.
- [63] Sugimoto, N. (2008). *Erbium Doped Fiber and Highly Non-Linear Fiber Based on Bismuth Oxide Glasses*. J. Non-Cryst. Solids, 354, 1205-1210.
- [64] Wang, Y. W. Hong, B. H., & Kim, K. S. (2005). *Size Control of Semimetal Bismuth Nanoparticles and the UV-Visible and IR Absorption Spectra*. J. Phys. Chem. B, 109, 7067-7072.
- [65] Wang, F., Tang, R., Yu, H., Gibbons, P. C., & Buhro, W. E. (2008). *Size- and Shape-Controlled Synthesis of Bismuth Nanoparticles*. Chem. Mater., 20, 3656-3662.
- [66] Zhang, Z. B., Gekhtman, D., Dresselhaus, M. S., Ying, J. Y. (1999). *Processing and Characterization of Single-Crystalline Ultrafine Bismuth Nanowires*. Chem. Mater., 11, 1659-1665.
- [67] Gao, Y., Niu, H., Zeng, C., Chen, Q. (2003). *Preparation and Characterization of Single-Crystalline Bismuth Nanowires by a Low-Temperature Solvothermal Process*. Chem. Phys. Lett., 367, 141-144.
- [68] Gekhtman, D., Zhang, Z. B., Adderton, D., Dresselhaus, M. S., & Dresselhaus, G. (1999). *Electrostatic Force Spectroscopy and Imaging of Bi Wires: Spatially Resolved Quantum Confinement*. Phys. Rev. Lett., 82, 3887-3890.
- [69] Kim, S. H., Choi, Y. S., Kang, K., & Yang, S. I. (2007). *Controlled Growth of Bismuth Nanoparticles by Electron Beam Irradiation in TEM*. J. Alloy. Compd., 427, 330-332.
- [70] Sepulveda-Guzman, S., Elizondo-Villarreal, N., Ferrer, D., Torres-Castro, A., Gao, X., Zhou, J. P., Jose-Yacaman, M. (2007). *In Situ Formation of Bismuth Nanoparticles Through Electron-Beam Irradiation in a Transmission Electron Microscope*. Nanotechnology, 18, 335604-1-6.
- [71] Kim, J. U., Cha, S. H., Shin, K., Jho, J. Y., & Lee, J. C. (2005). *Synthesis of Gold Nanoparticles from Gold (I)-Alkanethiolate Complexes with Supramolecular Structures through Electron Beam Irradiation in TEM*. J. Am. Chem. Soc., 127, 9962-9963.